The Journal of Experimental Life Science
OPEN ACCESS
p-ISSN: 2087-2852
e-ISSN: 2338-1655

RESEARCH ARTICLE

Hybrid VGG16–LSTM Classification of Microscopic Bacterial Images for Environmental Microbiology Screening

Indah Yanti [1]*, Marjono[1], Antariksa[2], Andi Kurniawan[3], Syaiful Anam[1], Hilmi Aziz Bukhori[1]

[1]Department of Mathematics, Faculty of Science, Technology and Mathematics, Universitas Brawijaya, Malang, 65145, Indonesia
[2]Department of Architecture, Faculty of Engineering, Universitas Brawijaya, Malang, 65145, Indonesia
[3]Department of Aquatic Resource Management, Faculty of Fisheries and Marine Science, Universitas Brawijaya, Malang, 65145, Indonesia

Correspondence:
Indah Yanti
Email : indah_yanti@ub.ac.id
Address : Universitas Brawijaya, Veteran Malang, 65145

Article History:
Submitted: 2026-02-18
Revised: 2026-06-11
Accepted: 2026-06-29
Available online: 2026-06-30

DOI: 10.21776/ub.jels.2026.016.02.02

Abstract

While conventional culture-based, biochemical, and molecular identification methods remain fundamental in microbiology, computational image analysis can serve as an exploratory, supplementary tool for studying bacterial morphology. This proof-of-concept study evaluates a hybrid VGG16-LSTM model for microscopic bacterial image classification. This study utilized a small subset of the DIBaS dataset consisting of six bacterial classes: *Acinetobacter baumannii*, *Escherichia coli*, *Lactobacillus plantarum*, *Micrococcus* spp., *Propionibacterium acnes*, and *Pseudomonas aeruginosa*. The total dataset size is highly constrained at 124 images, with a correspondingly small number of images per class ranging from 20 to 23. The dataset was divided into training, validation, and testing subsets in a 70:20:10 ratio. All microscopic images were resized to 224 × 224 pixels, normalized, and dynamically augmented during training to improve data variability under these limited-sample conditions. A pre-trained VGG16 network was employed to extract spatial image features, and the final convolutional feature map was reshaped into a spatial sequence and processed using an LSTM layer for further feature learning. Three optimization algorithms, namely Adam, RMSprop, and stochastic gradient descent, were compared. Among them, the RMSprop-optimized model exhibited the highest metrics after 50 epochs, achieving 92.86% accuracy, 95.24% precision, 92.86% recall, and a 92.38% F1-score; however, these performance indicators must be interpreted with caution as they are based on a severely limited test set (approximately 12 images). Some misclassifications occurred between *P. aeruginosa* and *E. coli*, which may be attributed to their shared gram-negative rod-shaped morphology. This finding highlights the inherent biological challenge of distinguishing visually similar bacterial species from microscopic image analysis alone, underscoring that such models remain strictly experimental and are not suited for clinical-grade diagnosis or field-ready environmental screening.

Keywords: bacterial classification; bioremediation; digital microscopy; environmental monitoring; VGG16-LSTM.

INTRODUCTION

Environmental pollution by petroleum hydrocarbons, pesticides, heavy metals, and other persistent pollutants remains a major ecological and public health concern. Conventional remediation approaches can be expensive, energy-intensive, and may cause secondary environmental impacts. Consequently, microbial bioremediation is increasingly recognized as a sustainable strategy. This is because microorganisms can transform, immobilize, degrade, or detoxify pollutants through diverse metabolic and enzymatic mechanisms [1-7]. In this context, the ability to recognize and monitor bacteria associated with environmental samples is an important step in microbial screening, contamination assessment, and bioremediation planning.

Bacteria contribute to bioremediation through their rapid growth, metabolic diversity, adaptability to environmental stressors, and ability to interact with pollutants. Genera such as

How to cite: Yanti, I., M. Marjono., A. Antariksa., A. Kurniawan., S. Anam., H. A. Bukhori. 2026. Hybrid VGG16-LSTM classification of microscopic bacterial images for environmental microbioogy screening. The Journal of Experimental Life Science, 16(2), 80-88. DOI: 10.21776/ub.jels.2026.016.02.02.

Pseudomonas, *Acinetobacter*, and *Micrococcus* have been associated with pollutant transformation, hydrocarbon degradation, metal tolerance, and survival in contaminated environments [3,5,7-13]. Other bacteria, including *Escherichia coli*, are important in environmental microbiology as indicators of fecal contamination and water quality risk [14]. Applied microbiology also includes bacteria relevant to biosorption, fermentation biotechnology, microbial safety, and comparative physiological studies, such as *Lactobacillus plantarum* and *Cutibacterium acnes* [15-18].

Despite the importance of bacterial identification, routine recognition remains challenging in laboratories with limited resources. Culture-based and biochemical methods are fundamental but often require repeated subculturing, multiple phenotypic tests, and expert interpretation [19,22]. Molecular methods can improve taxonomic resolution, but they are often more costly and may not be available for preliminary screening in small labs. These limitations create a need for complementary tools to support rapid, reproducible microscopic screening prior to confirmatory tests.

Digital microscopy offers a practical route for preliminary bacterial screening because microscopic images contain information on the cell shape, arrangement, staining pattern, texture, and local spatial organization. Manual interpretation of such images can be affected by subjectivity, observer fatigue, image quality, and similarity among the bacterial morphologies. Therefore, automated image-based analysis has become increasingly relevant in microbiology, particularly for microorganism detection, classification, and quantitative image interpretation [23,26].

Convolutional Neural Networks (CNNs) have been widely applied to microscopic image classification because they can learn spatial features directly from image data [23,26]. However, many machine learning studies emphasize algorithmic accuracy without adequately explaining the biological context of the selected organisms or the task's relevance to applied life sciences. For a journal in experimental life science, an image-classification model should be positioned not only as an artificial intelligence method but also as a microbiological support tool with a clear biological rationale and realistic boundaries of interpretation.

Fine-grained microscopic bacterial classification is biologically challenging because different taxa may share similar cell shapes and staining appearances. For example, *P. aeruginosa* and *E. coli* are Gram-negative rod-shaped bacteria that may display overlapping visual features under light microscopy [27]. A hybrid CNN-LSTM architecture may help address this challenge by combining CNN-based spatial feature extraction with LSTM-based learning over reshaped spatial feature sequences. In this design, VGG16 extracts local visual patterns, whereas the LSTM layer models dependencies across the sequence of feature vectors generated from the convolutional feature map [28,32-34].

This study aimed to develop and evaluate a VGG16-LSTM model as a complementary image-based screening tool for bacterial microscopic images relevant to applied microbiology, environmental monitoring, and preliminary bioremediation-oriented assessment. The study used selected classes from the DIBaS dataset [35] and compared Adam, RMSProp, and stochastic gradient descent (SGD) optimizers under small-sample learning conditions with on-the-fly augmentation. The model was not designed to replace culture-based biochemical, MALDI-TOF, or molecular identification methods. Instead, it was positioned as a preliminary decision-support approach that may help accelerate bacterial recognition in microbiology and environmental life science laboratories when rapid visual screening is needed.

MATERIAL AND METHOD

Dataset

This study used a subset of digital microscopic images of bacteria from the Digital Images of Bacteria Species (DIBaS) dataset [35]. The DIBaS dataset contains microscopic images of 33 bacterial species. Six classes were selected for the present study to represent biologically diverse bacteria relevant to environmental monitoring, applied microbiology, biotechnology, and comparative bacterial recognition. The selected classes included Gram-negative rods, Gram-positive rods, Gram-positive cocci, and aerotolerant anaerobic Gram-positive bacteria. The aim was not to claim that all selected bacteria are primary bioremediation agents but to develop an image-based screening framework across biologically diverse bacterial classes. However, in this study, particular emphasis was placed on bacterial species commonly associated with bioremediation (Table 1). To address this, we used a hybrid framework to experimentally investigate a Deep Learning approach.

Table 1. Composition of the bacterial colony image dataset

No	Genera	Species	Number of Images
1	*Acinetobacter*	*baumannii*	20
2	*Escherichia*	*coli*	20
3	*Lactobacillus*	*plantarum*	20
4	*Micrococcus*	*spp.*	21
5	*Propionibacterium*	*acnes*	23
6	*Pseudomonas*	*aeruginosa*	20

Sources: DIBaS dataset [35].

These research phases included dataset generation, image pre-processing with both the one-hot and RGB representations, and dynamic (on-the-fly) data augmentation for all experiments. Furthermore, we implemented a Hybrid VGG16-LSTM model and compared its performance against 3 various optimizers.

Data Preprocessing

The raw image dataset must undergo the following preprocessing before being fed as input to the model: Data Splitting to prevent data leakage among the training, validation, and test subsets, we followed the 70, 20, 10 rule. Training Set (70%): This was used to directly train the model's weights. Validation Set (20 %): This subset was used as the model benchmark during the training process, and Early Stopping was applied. Testing Set (10%): This was reserved for the final test of how well a trained model performed on new data. Image Normalization: The pixel values of the images were normalized from the original range [0, 255] to the standardized range [0, 1] to reduce the scale disparity for faster convergence of the gradient. Image Rescaling: All images were rescaled to 224×224 pixels, as per the input layer specifications of the VGG16 architecture.

Microscopic Data Augmentation Strategies

Because bacterial microscopic images generally do not have a fixed top–bottom or left–right orientation, horizontal and vertical flipping were considered biologically plausible augmentation operations. We used an On-the-fly Augmentation method. This processing method consists of the free production of manipulated images without generating additional storage files from a previous execution epoch. The augmentation parameters are Geometric Rotation (30°), to simulate the non-uniform orientation of small objects; Vertical and Horizontal Flip, as no “top” or “bottom” is defined in microscopic object and therefore in could be flipped; zoom range of up to 20%, to model variations on microscope lens magnifying capability; Brightness (0.8 1.2), due to the uneven intensity of microscope lamp; Shift & Shear reshaping position the image, relocating the object at different place.

Table 2. Sequential model

No	Layer (type)	Output Shape	Param#
1	input_layer (InputLayer)	(None, 224, 224, 3)	0
2	block1_conv1 (Conv2D)	(None, 224, 224, 64)	1,792
3	block1_conv2 (Conv2D)	(None, 224, 224, 64)	36,928
4	block1_pool (MaxPooling2D)	(None, 112, 112, 64)	0
5	block2_conv1 (Conv2D)	(None, 112, 112, 128)	73,856
6	block2_conv2 (Conv2D)	(None, 112, 112, 128)	147,584
7	block2_pool (MaxPooling2D)	(None, 56, 56, 128)	0
8	block3_conv1 (Conv2D)	(None, 56, 56, 256)	295,168
9	block3_conv2 (Conv2D)	(None, 56, 56, 256)	590,080
10	block3_conv3 (Conv2D)	(None, 56, 56, 256)	590,080
11	block3_pool (MaxPooling2D)	(None, 28, 28, 256)	0
12	block4_conv1 (Conv2D)	(None, 28, 28, 512)	1,180,160
13	block4_conv2 (Conv2D)	(None, 28, 28, 512)	2,359,808
14	block4_conv3 (Conv2D)	(None, 14, 14, 512)	2,359,808
15	block4_pool (MaxPooling2D)	(None, 14, 14, 512)	0
16	block5_conv1 (Conv2D)	(None, 14, 14, 512)	2,359,808
17	block5_conv2 (Conv2D)	(None, 14, 14, 512)	2,359,808
18	block5_conv3 (Conv2D)	(None, 14, 14, 512)	2,359,808
19	block5_pool (MaxPooling2D)	(None, 7, 7, 512)	0
20	reshape (Reshape)	(None, 49, 512)	0
21	lstm (LSTM)	(None, 128)	328,192
22	dropout (Dropout)	(None, 128)	0
23	dense (Dense)	(None, 64)	8,256
24	dropout_1 (Dropout)	(None, 64)	0
25	dense_1 (Dense)	(None, 6)	390

Hybrid Model Architecture (VGG16-LSTM)

The hybrid CNN-LSTM model is introduced by integrating the spatial feature-learning advantages of CNNs and the sequential processing advantages of LSTMs. A pre-trained VGG16 model with ImageNet weights was utilized as the base feature extractor. To preserve the generalized visual features learned from ImageNet and prevent overfitting, the entire VGG16 convolutional base was frozen (i.e., its layer weights were set to non-trainable). Consequently, only the weights of the newly appended LSTM layers were updated during the training process. The output from our final convolutional block, which has a shape of (7, 7, 512), is reshaped into a (49, 512) feature vector by a reshape layer. This vector is subsequently fed into the LSTM, treating the spatial side information as a continuous feature sequence.

Sequence Learning (RNN - LSTM)

A single LSTM unit with 128 neuron units was used to learn the feature correlations of VGG16. A Dropout (0.5) was set to prevent overfitting. The classifier (Fully Connected) was a 64-dense-layer ReLU. An output layer using softmax activation for multiclass categorization. The Hybrid model was experimentally tested under three optimization conditions with these hyperparameter values. For experimentation, they evaluated the hybrid model under three optimizer scenarios with such hyper-parametrization. Early Stopping was added to the training of the model by tracking the Validation Loss. After five passes without a reduction in the validation loss, training was stopped, and the best weights were returned.

RESULT

This section presents a comprehensive experimental evaluation of the proposed CNN–LSTM hybrid model (VGG16–LSTM), combined with on-the-fly data augmentation, for classifying microscopic images of bacteria. Given the limited number of samples per class (approximately 20 images), dynamic augmentation was employed during training to increase data variability, mitigate overfitting, and improve model generalization. The model performance was evaluated using three optimization algorithms, Adam, RMSProp, and Stochastic Gradient Descent (SGD), to identify the most effective optimization strategy under this small-sample learning regime.

The training stability and convergence behavior were analyzed using the validation accuracy and loss curves at training epochs 10, 20, 30, 40, and 50. As shown in Figure 1, each optimizer exhibits distinct learning dynamics when trained in conjunction with on-the-fly data augmentation.

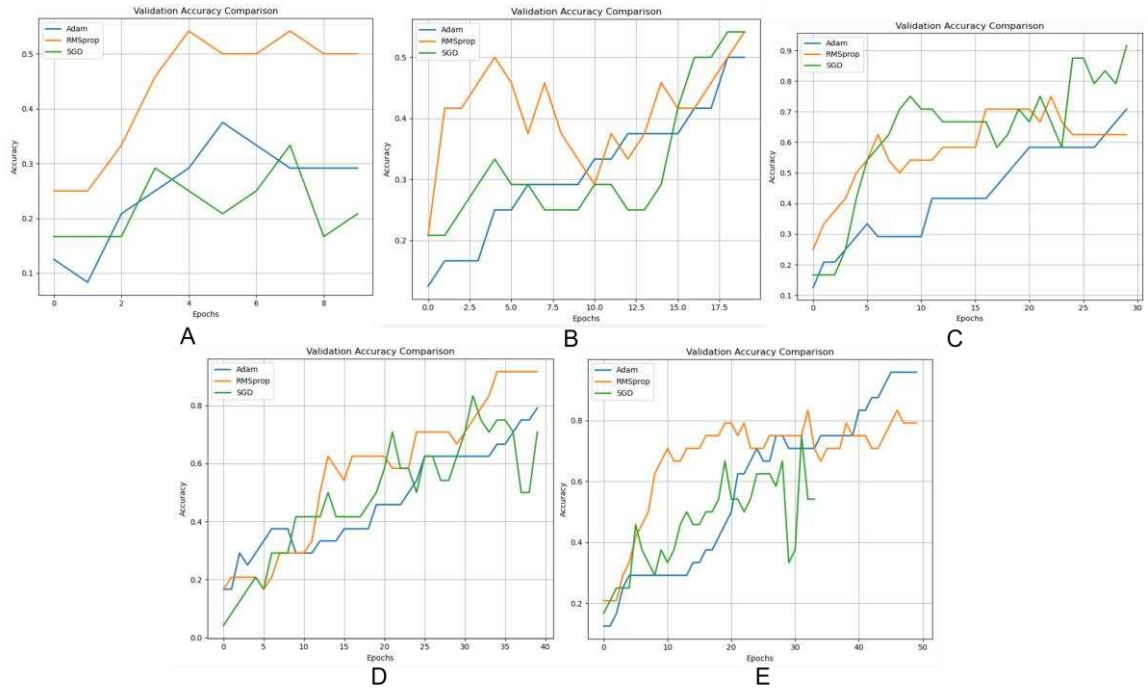

Figure 1. Validation Accuracy Comparison across Adam, RMSProp, and SGD Optimizers (A) epoch = 10; (B) epoch = 20; (C) epoch = 30; (D) epoch = 40; and (E) epoch = 50

The Adam optimizer demonstrated rapid performance improvement during the early training phase, reaching a validation accuracy above 80% by epoch 30. This behavior indicates that Adam benefits from the increased data variability introduced by on-the-fly augmentation, enabling fast adaptation to diverse augmented samples. However, after this point, the performance stagnated, and no further improvement was observed after epoch 50. This plateau suggests that Adam converges prematurely to a local minimum, potentially limiting its ability to exploit the additional augmented variations introduced in the later epochs.

In contrast, SGD exhibits pronounced instability throughout the training process, characterized by large oscillations in validation accuracy. A sharp drop in accuracy observed around epoch 40 (down to 64.29%) indicates an unstable gradient update. Despite the regularization effect of on-the-fly augmentation, SGD's fixed learning rate appears insufficient to handle the increased stochasticity of dynamically augmented inputs, leading to overshooting during optimization.

In contrast, RMSProp exhibited a gradual yet highly stable learning trajectory. Although its initial convergence rate is slower than that of Adam, RMSProp continuously benefits from the diversity of augmented samples and achieves a significant performance gain between epochs 30 and 40. Ultimately, RMSProp attained the highest and most s3 validation accuracy by the end of training, indicating superior compatibility with both the CNN–LSTM architecture and the on-the-fly augmentation strategy.

A quantitative comparison of the classification performance across epochs 10 to 50 is summarized in Table 3. The results clearly demonstrate that RMSProp is the most effective optimizer when combined with the VGG16–LSTM model and on-the-fly data augmentation. At epoch 50, RMSProp achieves the highest values across all evaluation metrics, including Accuracy (92.86%), Precision (95.24%), Recall (92.86%), and F1-score (92.38%). The consistently high F1-score indicates a balanced trade-off between precision and recall, confirming that the model generalizes well across bacterial classes despite the limited dataset size.

The model demonstrated a strong discriminative capability across most bacterial genera. Classes including *Acinetobacter baumannii*, *Lactobacillus plantarum*, *Micrococcus spp.*, and *Propionibacterium acnes* were classified with perfect accuracy, indicating that on-the-fly augmentation successfully enhanced feature robustness for these classes.

Minor misclassifications were observed in the *Pseudomonas aeruginosa* class, where a small number of samples were incorrectly predicted as *Escherichia coli*. This confusion is biologically plausible because both species are gram-negative, rod-shaped bacteria with highly similar microscopic morphologies. Even with dynamic augmentation, such subtle inter-class similarities remain challenging for CNN-based feature extractors, underscoring the intrinsic difficulty of fine-grained bacterial-image classification. The superior performance of RMSProp in this study can be attributed to its adaptive gradient normalization mechanism, which is particularly advantageous when training recurrent components, such as LSTM layers.

Table 3. Classification performance metrics across optimizers under On-the-Fly data augmentation

epoch	Optimizer	Accuracy	Precision	Recall	F1-Score
10	Adam	35.71	15.95	35.71	21.32
	RMSProp	50.00	46.94	50.00	44.44
	SGD	28.57	30.95	28.57	23.81
20	Adam	50.0	53.27	50.0	43.35
	RMSProp	50.0	39.29	50.0	41.43
	SGD	50.0	36.22	50.0	40.02
30	Adam	85.71	89.88	85.71	84.56
	RMSProp	71.43	71.79	71.43	65.82
	SGD	78.57	73.81	78.57	73.33
40	Adam	85.71	92.86	85.71	85.71
	RMSProp	92.86	95.24	92.86	92.38
	SGD	64.29	48.57	64.29	54.17
50	Adam	85.71	85.71	85.71	85.71
	RMSProp	**92.86**	**95.24**	**92.86**	**92.38**
	SGD	71.43	61.90	71.43	64.29

Source: Data processing, 2025

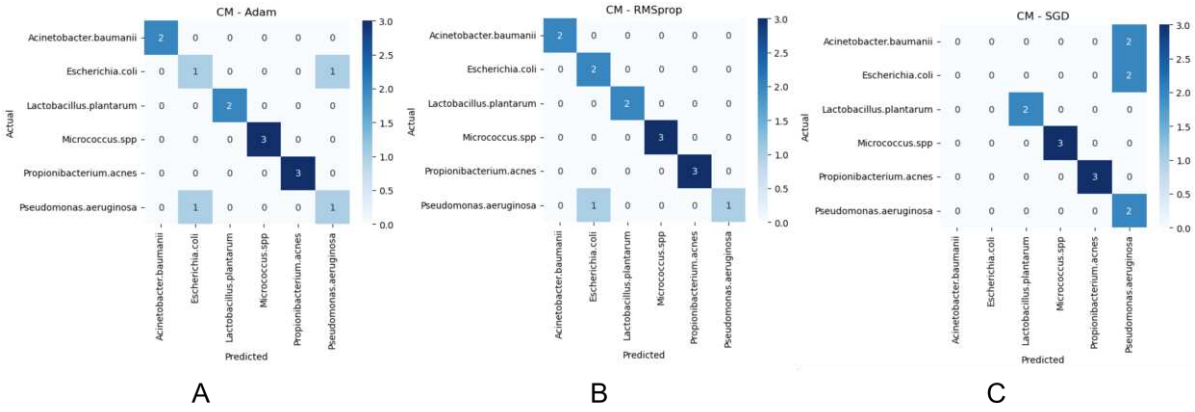

Figure 2. Confusion Matrix of the hybrid VGG16-LSTM model trained (epoch=50). (A) Adam; (B) RMSProp and; (C) SGD Optimizers

As shown in Figure 2, on-the-fly data augmentation introduces controlled stochasticity into the training process by presenting the model with a virtually unlimited set of biologically plausible variations. RMSProp effectively stabilizes gradient updates under this dynamic input distribution, thereby enabling a more efficient exploration of the loss landscape.

The premature convergence observed with Adam, despite its theoretical advantages, suggests that bias-corrected momentum may constrain parameter exploration when the training data distribution changes continuously due to on-the-fly augmentation. Consequently, Adam tends to converge early to suboptimal solutions in this small-sample scenario.

DISCUSSION

This study repositioned microscopic bacterial image classification as a support task for applied microbiology and environmental life science, rather than as a purely computational problem. The selected bacteria represent a mixture of environmentally relevant taxa, indicator organisms, and applied-microbiology classes. This design is important because an automated image-based system intended for environmental or bioremediation-oriented laboratories must be interpreted based on the biological properties of the organisms being classified. The strongest biological connection to bioremediation is provided by *Pseudomonas* spp., which are widely recognized for their metabolic versatility, hydrocarbon degradation, biosurfactant production, and survival in contaminated environments [8-10]. *Acinetobacter* spp. and *Micrococcus* spp. are also environmentally relevant because members of these genera have been detected in soil, wastewater, and polluted matrices and are associated with hydrocarbon degradation, biosurfactant activity, and heavy metal tolerance [10-13]. In contrast, *E. coli* is more appropriately interpreted as an environmental indicator and comparative Gram-negative rod than as a primary bioremediation organism [14]. *Lactobacillus plantarum* has applied-life-science relevance in fermentation biotechnology, probiotic applications, and biosorption-related metal binding [15,16]. *Propionibacterium acnes*, currently *C. acnes*, should be interpreted as a comparative Gram-positive aerotolerant anaerobe that increases physiological diversity rather than as a bioremediation agent [17,18].

From a modeling perspective, RMSProp exhibited the best performance and stability. RMSProp divides the gradient by a running average of recent gradient magnitudes, which can help stabilize the training when inputs vary dynamically owing to augmentation [36]. This behavior is particularly relevant when an LSTM layer is included, as its the recurrent components may be sensitive to unstable gradient updates. The final RMSProp performance of 92.86% accuracy and 92.38% F1-score suggests that the VGG16-LSTM architecture can extract useful microscopic features under limited-data conditions.

Adam showed faster early improvement but reached a performance plateau after epoch 30. This finding is consistent with reports that adaptive methods may converge quickly but do not always provide the best generalization in some non-convex learning tasks [37]. SGD showed the least stable performance, likely because its fixed-update behavior was less able to accommodate the stochasticity introduced by the on-the-fly augmentation. These differences indicate that the training strategy is important when microscopic datasets are small and dynamically augmented.

The misclassification between *Pseudomonas aeruginosa* and *Escherichia coli* was one of the most biologically informative findings of this study. Both species are Gram-negative rods and may share similar microscopic morphologies, especially when image quality, staining variation, and field-of-view differences are present [27]. This observation supports the argument that microscopic image-based classification should be used as a screening tool and not as a definitive taxonomic identification method. Confirmatory testing remains necessary, particularly when bacteria have similar morphologies or when species-level identification has clinical, environmental, or regulatory consequences.

Compared with standalone CNN-based approaches reported in bacterial or microorganism image studies, the VGG16-LSTM design may offer an advantage by allowing spatial dependencies in the convolutional feature map to be learned as a sequence [26,33,34]. On-the-fly augmentation also reduces the risk of memorizing a small fixed set of transformed images, a problem noted in image augmentation studies involving limited datasets [38]. Nevertheless, the performance must be interpreted with caution because the original dataset was small and did not capture the full variability of environmental isolates.

Overall, the results support the feasibility of using hybrid image-based learning as a complementary tool for preliminary bacterial screening in applied microbiology. In a bioremediation-oriented workflow, such a system could help prioritize candidate images or guide early recognition before biochemical and molecular confirmation. However, its practical value will depend on validation across larger datasets, multiple laboratories, environmental samples, and different staining protocols, as well as bacteria isolated from contaminated sites.

CONCLUSION

This study evaluated a hybrid VGG16-LSTM model with on-the-fly data augmentation as a complementary image-based approach for preliminary bacterial screening in applied microbiology, environmental monitoring, and bioremediation-oriented assessment. The selected bacterial classes represented environmentally relevant taxa, indicator organisms, biotechnology-related species, and comparative microscopic classes, thereby supporting the study's applied life-science relevance.

Among the three optimizers tested, RMSProp achieved the best performance after 50 epochs, with 92.86% accuracy, 95.24% precision, 92.86% recall, and a 92.38% F1-score. These results indicate that the proposed model can extract useful microscopic features from limited bacterial image data.

Misclassification between *P. aeruginosa* and *E. coli* reflects the biological difficulty of distinguishing visually similar Gram-negative rod-shaped bacteria using microscopic images alone. Therefore, the model should be interpreted as a preliminary screening and decision-support tool, not as a replacement for culture-based, biochemical, MALDI-TOF, or molecular identification methods.

Overall, the proposed framework shows potential to support early bacterial recognition in applied microbiology and environmental life sciences laboratories. Further validation using larger datasets, environmental isolates, different staining protocols, and multi-laboratory imaging conditions is required before practical implementation in bioremediation-related workflows.

Author Contribution: IY: Conceptualization, Writing–Original Draft, Methodology, Software, Project Administration. M: Validation, Writing–Review and Supervision. A: Methodology. AK: Methodology, Conceptualization, Validation, Writing–Review, Editing, and Supervision. SA: Conceptualization, Validation, Resources, Writing–Review, Editing, Supervision, Software, and Formal Analysis. HAB: Software, and Formal Analysis.

Funding: This research was funded by the Faculty of Sciences, Technology, and Mathematics, grant number 02115.05/UN10.F09/PN/2025.

Conflict of Interest: The authors have no conflict of interest.

REFERENCES

[1]. Abdelhamid, M.A.A., H.O. Khalifa., H.J. Yoon, MR. Ki, S.P. Pack. 2024. Microbial immobilized enzyme biocatalysts for multipollutant mitigation: Harnessing nature's toolkit for environmental sustainability. *Int. J. Mol. Sci*. 25(16). 8616. DOI: 10.3390/ijms25168616.

[2]. Ali, S.S., L.H.S. Hassan, M. El-Sheekh. 2024. Microalgae-mediated bioremediation: Current trends and opportunities-a review.

Arch. Microbiol. 206(8). 343. DOI: 10.1007/s00203-024-04052-x.

[3]. Kour, D., T. Kaur, R. Devi, A. Yadav, M. Singh, *et al*. 2021. Beneficial microbiomes for bioremediation of diverse contaminated environments for environmental sustainability: Present status and future challenges. *Environ. Sci. Pollut. Res*. 28(20). 24917-24939. DOI: 10.1007/s11356-021-13252-7

[4]. Maglione, G., P. Zinno, A. Tropea, C.U. Mussagy, L. Dufosse, *et al*. 2024. Microbes' role in environmental pollution and remediation: A bioeconomy focus approach. *AIMS Microbiol*. 10(3). 723-755. DOI: 10.3934/microbiol.2024033

[5]. Manikandan, S.K., P. Pallavi, K. Shetty, D. Bhattacharjee, D.A. Giannakoudakis, *et al* 2023. Effective usage of biochar and microorganisms for the removal of heavy metal ions and pesticides. *Molecules*. 28(2). 719. DOI: 10.3390/molecules28020719.

[6]. Nguyen, N.T., V.T. Vo, T.H.P. Nguyen, R. Kiefer. 2022. Isolation and optimization of a glyphosate-degrading *Rhodococcus soli* G41 for bioremediation. *Arch. Microbiol*. 204, 252. DOI: 10.1007/s00203-022-02875-0

[7]. Salari, M., V. Rahmanian, S.A. Hashemi, W-H. Chiang, C.W. Lai, *et al*. 2022. Bioremediation treatment of polyaromatic hydrocarbons for environmental sustainability. *Water*. 14(23). 3980. DOI: 10.3390/w14233980

[8]. Abdoli, S., B.A. Lajayer, S.B. Novair, G.W. Price. 2025. Unlocking the potential of biosurfactants in agriculture and environmental remediation: Novel applications and future directions. *Sustainability*. 17(5). DOI: 10.3390/su17052110.

[9]. Babayola, N. M., M.A. Adefisoye. 2025. Recent advances and prospects of microbial biosurfactant-mediated remediation of engine oil pollution: A comprehensive review. *Nat. Environ. Pollut. Technol.* 24(1). 1–15. DOI: 10.46488/NEPT.2025.v24i01.D1655.

[10]. Babayola, N.M., N.B. Lecky, C.O. Onumaegbu, O.O. Olayujigbe, M.A. Adefisoye. 2026. Assessment of the bioremediation potentials of biosurfactant-producing bacterial strains recovered from spent engine oil-contaminated environments in southwest Nigeria. *J. Environ. Sci. Sustain. Dev.* 9(1). 111-128. DOI: 10.7454/jessd.v9i1.1415.

[11]. Parthipan, P., L. Cheng, A. Rajasekar, O.P. Karthikeyan, P.K.S.M. Rahman. 2024. Editorial: Biosurfactants - next-generation biomolecules for enhanced biodegradation of organic pollutants, volume II. *Front. Microbiol.* 12.015.01513087. DOI: 10.3389/fmicb.2024.1513087.

[12]. Ezeonuegbu, B.A., C.C. Nwankwo, G.F. Dappa. 2024. Heavy metal co-resistance with antibiotics amongst plant growth promoting bacteria isolates from rhizosphere of *Nypa fruticans*. *Int. J. Res. Sci. Innov*. 11(5). 379-394. DOI: 10.51244/IJRSI.2024.1105024.

[13]. Mekonnen, B. A., T.A. Aragaw, M.B. Genet. 2024. Bioremediation of petroleum hydrocarbon contaminated soil: A review on principles, degradation mechanisms, and advancements. *Front. Environ.l Sci*. 12. 1354422. DOI: 10.3389/fenvs.2024.1354422

[14]. World Health Organization. 2022. *Guidelines for drinking-water quality: Fourth edition incorporating the first and second addenda*. World Health Organization. Available at: https://www.who.int/publications/i/item/9789240045064.

[15]. Kumar, R., T.P. Vasić, S.P. Živković, P. Panneerselvam, G. Santoyo, *et al.* 2025. Mechanistic role of heavy metals in driving antimicrobial resistance: From rhizosphere to phyllosphere. *Appl. Microbiol*. *5*(3). 79. DOI: 10.3390/applmicrobiol5030079.

[16]. Gillieatt, B.F., N.V. Coleman. 2024. Unraveling the mechanisms of antibiotic and heavy metal resistance co-selection in environmental bacteria. *FEMS Microbiol. Rev.* 48. fuae017. DOI: 10.1093/femsre/fuae017.

[17]. Mias, C., V. Mengeaud, S. Bessou-Touya, H. Duplan. 2023. Recent advances in understanding inflammatory acne: Deciphering the relationship between *Cutibacterium acnes* and Th17 inflammatory pathway. *J. Eur. Acad. Dermatol. Venereol.* 37(2). 3-11. DOI: 10.1111/jdv.18794.

[18]. Smythe, P., H.N. Wilkinson. 2023. The skin microbiome: Current landscape and future opportunities. *Int. J. Mol. Sci*. 24(4). DOI: 10.3390/ijms24043950.

[19]. Gopal, A., L. Yan, S. Kashif, T. Munshi, V.A. Roy, N.H. Voelcker, X. Chen. 2022. Biosensors and point-of-care devices for bacterial detection: Rapid diagnostics informing antibiotic therapy. *Adv. Healthc. Mater*. 11(3). DOI: 10.1002/adhm.202101546.

[20]. Corvec, S., M.A. Dagnelie, A. Khammari, B. Dreno. 2019. Taxonomy and phylogeny of *Cutibacterium* (formerly *Propionibacterium*) *acnes* in inflammatory skin diseases. *Ann. Dermatol. Venereol*. 146(1). 26-30. DOI: 10.1016/j.annder.2018.11.002.

[21]. Samarasinghe, S.N., D.N. Magana-Arachchi, R.P. Wanigatunge. 2021. Bacterial diversity in a Sri Lankan geothermal spring assessed by culture-dependent and culture-independent approaches. *Curr. Microbiol*. 78(9). DOI: 10.1007/s00284-021-02608-4.

[22]. Singh, S., S. Rao, D.K. Saini, S.J. Venugopal, P.T. Rekha, S. Umapathy, D. Reghu, S. Mohandas, D. Kumbhar, S.K. Chunchanur, A. Rangaiah. 2022. Culture-independent Raman spectroscopic identification of bacterial pathogens from clinical samples using deep transfer learning. *Anal. Chem*. 94(42). 14745-14754. DOI: 10.1021/acs.analchem.2c03391.

[23]. Ma, H., Y. Su, S. Qiao, X. Jiang, X. Chen, J. Yang, G. Zhong. 2021. Deep convolutional neural network: A novel approach for the detection of *Aspergillus* fungi via stereomicroscopy. *J. Microbiol*. 59(6). 563-572. DOI: 10.1007/s12275-021-1013-z.

[24]. Yilmaz, A., F. Goktay, R. Varol, G. Gencoglan, H. Uvet. 2022. Deep convolutional neural networks for onychomycosis detection using microscopic images with KOH examination. *Mycoses.* 65(12). 1119-1126. DOI: 10.1111/myc.13498.

[25]. Ma, P., C. Li, M.M. Rahaman, Y. Yao, J. Zhang, S. Zou, *et al.* 2023. A state-of-the-art survey of object detection techniques in microorganism image analysis: From classical methods to deep learning approaches. *Artif. Intell. Rev*. 56(2). 1627-1698. DOI: 10.1007/s10462-022-10209-1.

[26]. Rani, P., V. Sharma, S. Kotwal, J. Manhas, S. Sharma. 2021. Machine learning and deep learning based computational approaches in automatic microorganisms image recognition: Methodologies, challenges, and developments. *Arch. Comput. Methods Eng*. 29(3). 1801-1837. DOI: 10.1007/s11831-021-09639-x.

[27]. Madigan, M.T., K.S. Bender, D.H. Buckley, W.M. Sattley, D.A. Stahl. 2021. Brock biology of microorganisms. 16th Ed. Pearson.

[28]. Srikantamurthy, M.M., S. Natarajan, V.P.S. Rallabandi, D.B. Dudekula, J. Park. 2023. Classification of benign and malignant subtypes of breast cancer histopathology imaging using hybrid CNN-LSTM based transfer learning. *BMC Med. Imaging*. 23(1), 19. DOI: 10.1186/s12880-023-00964-0.

[29]. Wahid, A., J.G. Breslin, M.A. Intizar. 2022. Prediction of machine failure in industry 4.0: A hybrid CNN-LSTM framework. *Appl. Sci*. 12(9). 4221. DOI: 10.3390/app12094221.

[30]. Gomez-de-Mariscal, E., G. Garcia-Rojo, W. Ouyang, *et al.* 2021. DeepImageJ: A user-friendly environment to run deep learning models in ImageJ. *Nat. Methods*. 18. 1192-1195. DOI: 10.1038/s41592-021-01262-9.

[31]. Lundervold, A.S., A. Lundervold. 2022. An overview of deep learning in medical imaging focusing on MRI and microscopy data. *Z Med Phys*. 29(2). 102-127. DOI: 10.1016/j.zemedi.2018.11.002.

[32]. Graham, S., Q.D. Vu, S.E. A. Raza, A. Azam, et al. 2021. HoVer-Net: Simultaneous segmentation and classification of nuclei in multi-tissue histology images. *Med. Image Anal*. 58. 101563. DOI: 10.1016/j.media.2019.101563.

[33]. Bukhari, M., S. Yasmin, S. Sammad, A.A.A. El-Latif. 2022. A deep learning framework for leukemia cancer detection in microscopic blood samples using squeeze and excitation learning. *Math. Probl. Eng.* 1. 2801227. DOI: 10.1155/2022/2801227.

[34]. Greff, K., R.K. Srivastava, J. Koutnik, B.R. Steunebrink, J. Schmidhuber. 2017. LSTM: A search space odyssey. *IEEE Trans. Neural Netw. Learn. Syst.* 28(10). 2222-2232. DOI: 10.1109/TNNLS.2016.2582924

[35]. Zielinski, B., A. Plichta, K. Misztal, P. Spurek, M. Brzychczy-Wloch, D. Ochonska. 2017. Deep learning approach to bacterial colony classification. *PLOS ONE*. 12(9). e0184554. DOI: 10.1371/journal.pone.0184554.

[36]. Zhang, A., Z.C. Lipton, M. Li, A.J. Smola. 2023. Dive into deep learning. Cambridge University Press.

[37]. Wilson, A.C., R. Roelofs, M. Stern, N. Srebro, B. Recht. 2017. The marginal value of adaptive gradient methods in machine learning. *Adv. Neural Inf. Process. Syst*. 30. DOI: 10.48550/arXiv.1705.08292.

[38]. Mumuni, A., F. Mumuni. 2022. Data augmentation: A comprehensive survey of modern approaches for deep learning image analysis. *Array*. 16. 100258. DOI: 10.1016/j.array.2022.100258.